

# Transition Metal Complexes of 2-Acetylpyridine *o*-Hydroxybenzoylhydrazone (APo-OHBH): Their Preparation, Characterisation and Antimicrobial Activity

Nagwa NAWAR\* and Nasser Mohamed HOSNY

Chemistry Department, Faculty of Science, Mansoura University, Mansoura 35516, P. O. Box 79, Egypt.

Received January 25, 1999; accepted April 17, 1999

Coordination compounds of some transition metal ions with 2-acetylpyridine-*o*-hydroxybenzoylhydrazone (APo-OHBH) were synthesized. Their structures have been characterised by elemental analyses, electrical conductance, magnetic moments (at 25 °C) and spectral (IR, UV, NMR) studies. The fast atom bombardment (FAB) method was used for obtaining mass spectra of the positive ion FAB studies of the ligand and some metal complexes. The thermal behaviour of selected complexes was investigated by thermal gravimetric analysis (TGA) and differential thermal analysis (DTA) techniques. The IR spectra show that the ligand acts in a neutral bidentate, neutral tridentate and/or mononegative tridentate fashion depending on the metal salt used and the medium of the reaction. Preliminary pharmacological tests on the ligand and its complexes showed some antimicrobial activity.

**Key words** antimicrobial activity; hydrazone complexes; transition metal complexes

Interest in the studies of hydrazides and their corresponding hydrazones arises from the fact that hydrazides of organic acids and their hydrazones can function as antituberculous compounds.<sup>1)</sup> The antituberculous activity of hydrazides was ascribed to their ability to form more or less stable chelates with the transition metal ions.<sup>2,3)</sup>

The chemistry of transition metal complexes of hydrazones continues to be of interest on account of the interesting structural features presented by this class of compounds and also because of their biological importance.<sup>4–11)</sup> All this information stands as a testimony to the versatility of the hydrazones as chelating agents. In continuation of our previous studies on metal complexes of *o*-aminoacetophenone benzoylhydrazone (AABH)<sup>12)</sup> and *o*-aminoacetophenone-*o*-hydroxybenzoylhydrazone (AAOHBH),<sup>13)</sup> we describe here the synthesis, spectral, magnetic properties and antimicrobial activity of some metal complexes with 2-acetylpyridine-*o*-hydroxybenzoylhydrazone (APo-OHBH). Also, the fast atom bombardment (FAB) method was used for obtaining mass spectra of involatile species. In this paper, we focus on positive ion FAB studies of the ligand and some metal complexes and antimicrobial activity.

## Experimental

**Materials** Reagent grade chemicals were used without further purification.

**Physical Measurements** The metals were determined by complexometric titration against EDTA.<sup>14)</sup> Carbon, hydrogen and nitrogen contents were determined by the Microanalytical Unit of Liverpool University. Characterisation of the complexes was accomplished using a Pye Unicam SP 8800 spectrophotometer. Magnetic moments were determined by a Johnson Matthey magnetic susceptibility balance. The IR spectra of the ligand and its metal complexes were made in KBr pellets on a Mattson 5000 FTIR spectrometer. Calibration of the frequency reading was made with polystyrene film. The electronic spectra in dimethyl sulfoxide (DMSO) were made with a Unicam UV/Vis. spectrometer UV2 using 1 cm stoppered silica cells. Molar conductivities in DMSO ( $10^{-3}$  mol l<sup>-1</sup>) at room temperature (25 °C) were measured using a Hanna Model conductivity bridge. <sup>1</sup>H-NMR spectra were recorded at ambient temperature on a Bruker WM250 multinuclear spectrometer (University of Liverpool). FAB mass spectra were recorded at 70 eV on a VG 7070 EEC spectrometer (University of Liverpool). Thermal analyses were measured on the TGA-50 and DTA-50 Shimadzu differential

thermal analyser. The water of hydration was determined by heating the hydrated complexes up to 120 °C and then determining the loss in weight.

**Preparation of Ligand** The ligand was prepared by refluxing equimolar mixtures of 2-acetylpyridine (5.6 ml, 0.05 mol) and *o*-hydroxybenzoylhydrazine (7.0 g, 0.05 mol) in 50 ml absolute ethanol in a water bath for 6 h. The isolated compound was filtered off as yellow crystals, washed with ethyl alcohol, recrystallised from absolute ethanol and finally dried in a vacuum desiccator over anhydrous calcium chloride (yield 11.0 g, 80.0%, mp 238 °C).

**Preparation of Complexes** The metal complexes were prepared by adding stoichiometric quantities (0.3 mmol) of the hydrated metal(II) salts, e.g., chloride and acetate in 50 ml absolute ethanol to the ligand (0.3 mmol) in 50 ml absolute ethanol. The mixtures were refluxed in a water bath for about 3–6 h. Mono-ligand complexes were obtained by mixing equimolar amounts of ligand and metal salts, whereas bis-ligand complexes of NiCl<sub>2</sub>·H<sub>2</sub>O were separated out when excess of the ligand had been added. The isolated metal complexes were washed several times with hot ethanol and diethylether and finally dried in a vacuum desiccator over anhydrous calcium chloride. All the isolated complexes were insoluble in most organic solvents with melting point above 300 °C.

**Antimicrobial Activity** The antimicrobial activity of the ligand (APo-OHBH) and the complexes against *Escherichia coli* and *Bacillus subtilis* were determined using the cup-diffusion method.<sup>15)</sup> Each of the compounds was dissolved in dimethylformamide (DMF) and a solution with the concentration 500 μg ml<sup>-1</sup> was prepared.

## Results and Discussion

All the complexes are coloured and stable on prolonged exposure in air. They are soluble in coordinating solvents such as DMF and DMSO, but insoluble in other common organic solvents. Molar conductivities in  $1 \times 10^{-3}$  molar DMF at 25 °C (Table 1) show a 1 : 1 electrolytic nature of the [MLCl]Cl (M=Mn(II), Co(II) or Ni(II)) complexes and a nonionic behaviour for the rest.<sup>16)</sup> Elemental analyses and other physical data are presented in Table 1.

Five types of complexes, i.e. [Cu(L-H)OAc]; [M(L-H)<sub>2</sub>]·nH<sub>2</sub>O (where M=Cu(II), Ni(II) or Cd(II) and n=0–2); [MLCl]Cl (where M=Mn(II), Co(II) or Ni(II)); [MLCl<sub>2</sub>] (where M=Cu(II) or Hg(II)) and [Fe(L-H)Cl<sub>2</sub>] were formed from different ions, and can be explained by the fact that the ligand coordinates not only as mono-(HL<sup>-</sup>) and divalent (L<sup>2-</sup>) anions, but also in a tridentate.

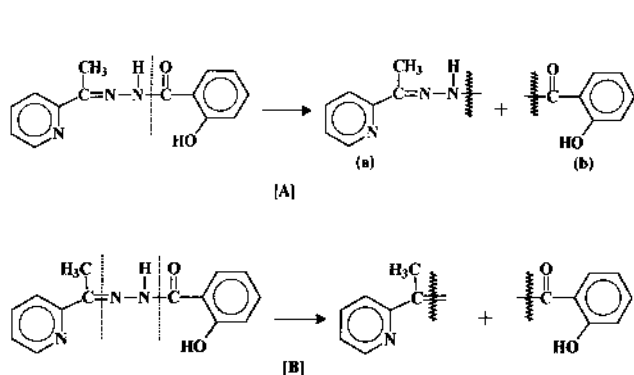
**Mass Spectra** Analysis by FAB mass spectroscopy gave

\* To whom correspondence should be addressed.

Table 1. Analytical and Physical Data for the Complexes Derived from APo-OHBH

| Compound                                  | Empirical formula   | Yield (%) | mp (°C) | Colour             | Found (Calcd) %  |                 |                  |                  |                  | $\Lambda_m^{(a)}$<br>DMSO |
|---|---|-----------|---------|--------------------|------------------|-----------------|------------------|------------------|------------------|---------------------------|
|   |   |           |         |                    | C                | H               | N                | M                | X                |                           |
| L=APo-OHBH                                | C <sub>14</sub> H <sub>13</sub> N <sub>3</sub> O <sub>2</sub>                   | 79        | 238     | Yellow             | 56.8<br>(56.83)  | 5.09<br>(5.09)  | 16.48<br>(16.47) | —                | —                | —                         |
| [Cu(L-H)OAc]                              | CuC <sub>16</sub> H <sub>15</sub> N <sub>3</sub> O <sub>2</sub>                 | 49        | >300    | Green              | 50.66<br>(50.8)  | 4.40<br>(4.20)  | 11.11<br>(11.10) | 16.75<br>(16.80) | —                | 5.0                       |
| [Co(L-H) <sub>2</sub> ]·2H <sub>2</sub> O | CoC <sub>28</sub> H <sub>32</sub> N <sub>6</sub> O <sub>6</sub>                 | 53        | >300    | Reddish<br>brown   | 56.0<br>(55.8)   | 4.23<br>(4.80)  | 13.72<br>(13.90) | 10.30<br>(10.00) | —                | 4.5                       |
| [Ni(L-H) <sub>2</sub> ]                   | NiC <sub>28</sub> H <sub>32</sub> N <sub>6</sub> O <sub>4</sub>                 | 68        | >300    | Reddish<br>brown   | 59.4<br>(59.29)  | 4.49<br>(4.23)  | 14.89<br>(14.82) | 9.80<br>(10.35)  | —                | 7.0                       |
| [Cu(L-H) <sub>2</sub> ]                   | CuC <sub>28</sub> H <sub>24</sub> N <sub>6</sub> O <sub>4</sub>                 | 65        | >300    | Green              | 58.57<br>(58.84) | 4.10<br>(4.20)  | 14.84<br>(14.71) | 10.80<br>(11.03) | —                | 9.0                       |
| [Cd(L-H) <sub>2</sub> ]                   | CdC <sub>28</sub> H <sub>24</sub> N <sub>6</sub> O <sub>4</sub>                 | 63        | >300    | Yellow             | 28.24<br>(28.54) | 4.20<br>(3.96)  | 13.89<br>(13.50) | 17.80<br>(18.07) | —                | 5.0                       |
| [MnLCl]Cl                                 | MnC <sub>14</sub> H <sub>13</sub> N <sub>3</sub> O <sub>2</sub> Cl <sub>2</sub> | 76        | >300    | Yellow             | 44.20<br>(43.99) | 3.52<br>(3.40)  | 11.33<br>(10.99) | 14.82<br>(14.63) | 18.40<br>(18.59) | 50                        |
| [CoLCl]Cl                                 | CoC <sub>14</sub> H <sub>13</sub> N <sub>3</sub> O <sub>2</sub> Cl <sub>2</sub> | 64        | >300    | Green              | 44.03<br>(43.76) | 3.40<br>(3.38)  | 10.80<br>(10.94) | 15.50<br>(15.08) | 18.20<br>(18.49) | 50                        |
| [NiLCl]Cl                                 | NiC <sub>14</sub> H <sub>13</sub> N <sub>3</sub> O <sub>2</sub> Cl <sub>2</sub> | 58        | >300    | Green              | 43.64<br>(43.67) | 2.46<br>(2.47)  | 11.33<br>(10.91) | 14.32<br>(15.25) | 18.20<br>(18.45) | 50                        |
| [CuLCl <sub>2</sub> ]                     | CuC <sub>14</sub> H <sub>13</sub> N <sub>3</sub> O <sub>2</sub> Cl <sub>2</sub> | 77        | >300    | Green              | 43.41<br>(43.13) | 3.42<br>(3.33)  | 10.98<br>(10.78) | 15.60<br>(16.29) | 17.70<br>(18.23) | 2.0                       |
| [Fe(L-H)Cl <sub>2</sub> ]                 | FeC <sub>14</sub> H <sub>12</sub> N <sub>3</sub> O <sub>2</sub> Cl <sub>2</sub> | 30        | >300    | Brown              | 44.05<br>(43.97) | 3.16<br>(3.40)  | 11.33<br>(10.99) | 14.20<br>(14.66) | 18.00<br>(18.58) | 9.0                       |
| [HgLCl <sub>2</sub> ]                     | HgC <sub>14</sub> H <sub>13</sub> N <sub>3</sub> O <sub>2</sub> Cl <sub>2</sub> | 80        | >300    | Yellowish<br>white | 31.88<br>(31.90) | 2.48<br>(45.14) | 8.00<br>(7.97)   | 38.00<br>(38.08) | 12.60<br>(13.48) | 4.5                       |

a)  $\text{ohm}^{-1} \text{cm}^2 \text{mol}^{-1}$ .



the molecular ion  $[M^+]$  of the ligand (APo-OHBH) which has strong intensity peak (100%) at the desired position  $m/z=256$ . The mass spectra of the ligand under investigation are recorded in Chart 1. Two major fragmentation pathways are followed by the molecular ion of (APo-OHBH) ligand. The first one [A], includes an ion peak at  $m/z=121$  (43.56%). This can be ascribed to the fragment ion (a)  $m/z=134$  (17.44%) resulting from the elimination of benzoyl fragment (b).

The second one [B], includes the cleavage occurring on  $-N-C-$  and  $-C=N-$  by elimination of the diazo group. This can be attributed to the fragment ions  $m/z=121$  (b) and  $m/z=106$  as shown in Chart 1. The benzoyl fragment was more abundant than the diazo cleavage.

There is also evidence in which the pyridine fragment removed from the molecular ion of the ligand and observed at the desired position  $m/z=177$ . The fragmentation patterns for the ligand (APo-OHBH) were as follows:

Analysis by FAB mass spectroscopy gave the molecular ion of the  $[\text{Ni}(\text{L-H})_2]$ ,  $[\text{Cu}(\text{L-H})_2]$  and  $[\text{Cd}(\text{L-H})_2]$  complexes at the desired position  $m/z=567$ , 572, and 623, re-

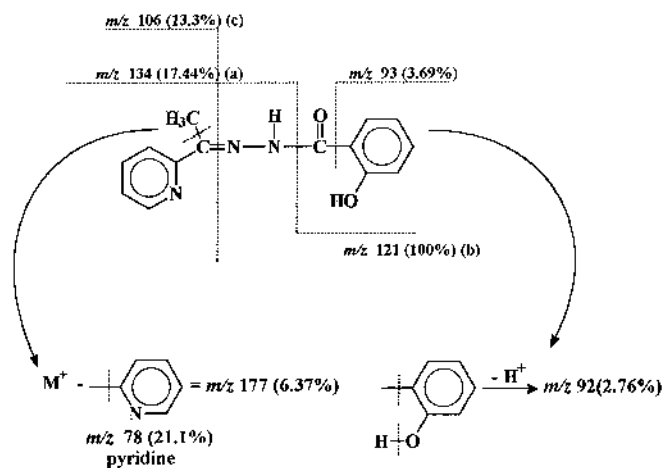


Chart 1. Proposed Fragmentation Route of APo-OHBH Ligand

spectively. Two major fragmentation pathways are followed by the molecular ion of the complexes as shown in Chart 2. The fragmentation of molecular ion of ligated nickel, copper and cadmium complexes occurs mainly because of the initial loss of phenol radical from one ligand moiety to give a fragment at  $m/z=473$ , 478, and 530, respectively. The resulting fragments lose another phenol radical. A pyridine radical is ejected from the last fragment to afford the species  $m/z=303$  for Ni and 308 for Cu followed by loss of another pyridine radical, and then the metal atom as shown in Chart 2. In the case of cadmium, a peak at  $m/z=423$  was observed due to the loss of methyl molecule. The other route includes an ion peak at  $m/z=317$  resulting from the elimination of ligand ion.

The fragmentation of ligated nickel and copper chloride complexes occurs primarily due to initial loss of chlorine

atom, and then metal atom as shown in Chart 3. This can be ascribed to the fragment ion  $m/z=348$  for nickel and  $m/z=353$  for copper complexes. After losing the metal, the molecular ion of the ligand appears at  $m/z=256$ . The fragmentation of the ligand ion occurs *via* carbon–amide nitrogen cleavage. This cleavage results in the ion peak at  $m/z=121$  (100%).

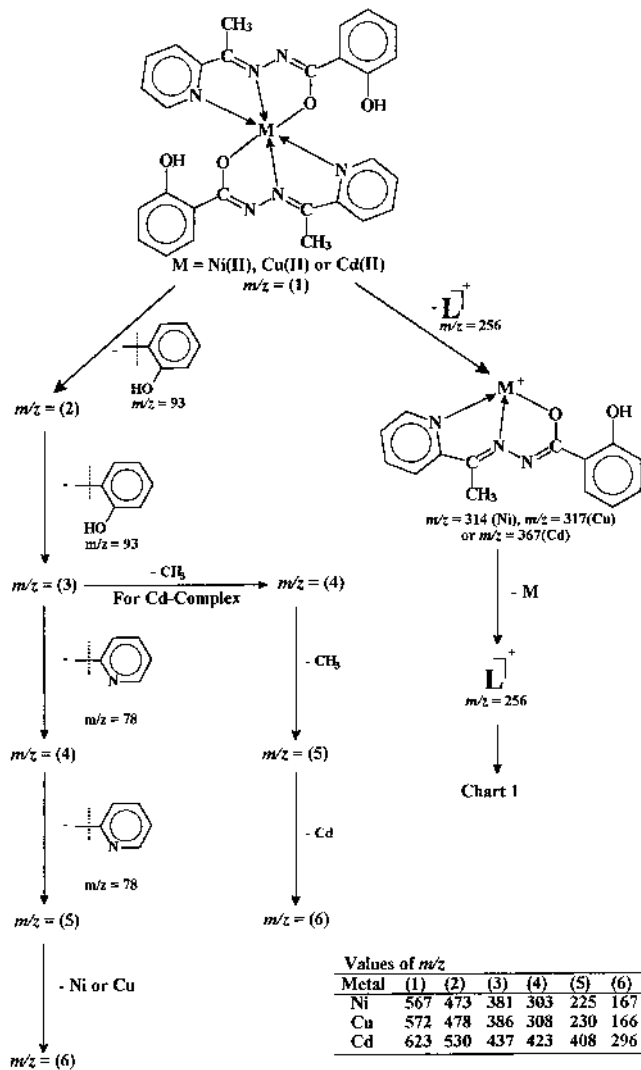


Chart 2. Proposed Fragmentation Route of  $[\text{Ni}(\text{L}-\text{H})_2]$ ,  $[\text{Cu}(\text{L}-\text{H})_2]$  or  $[\text{Cd}(\text{L}-\text{H})_2]$  Complexes

**$^1\text{H-NMR}$  and IR Spectra** The  $^1\text{H-NMR}$  spectrum of the ligand in  $d_6$ -DMSO exhibits two signals at 11.83 and 11.48 ppm relative to tetramethylsilane (TMS). These signals are assigned to the OH and NH protons, respectively. The presence of the NH proton downfield region may be due to the involvement of this group in hydrogen bonding with  $d_6$ -DMSO. The presence of NH signal indicates the presence of APo-OHBH in the keto form. The multisignals within the range 7.0–8.80 ppm are assigned to the aromatic protons of both rings.<sup>17</sup> The signal at 2.35 ppm is assigned to the  $\text{CH}_3$  group. The  $^1\text{H-NMR}$  spectra of the  $[\text{HgLCl}_2]$  and  $[\text{Cd}(\text{L}-\text{H})_2]$  complexes in  $d_6$ -DMSO show a negative shift of the signal due to the NH group, downfield of TMS. This signal is observed at 11.7 ppm for the Cd(II) complex while at 11.57 ppm for the Hg(II) complex, suggesting that the coordination proceeds through the carbonyl oxygen or azomethine nitrogen groups.<sup>18,19</sup> The downfield shifts of the methyl group signals at 2.58 ppm for the Cd(II) and at 2.55 ppm for the Hg(II) complexes, support the coordination *via* the azomethine nitrogen.

The IR band assignments are included in Table 2. The IR spectrum of the ligand shows a broad band at  $2445\text{ cm}^{-1}$  which may be assigned to  $\text{OH}\cdots\text{O}$  stretching vibration and indicates the presence of intramolecular hydrogen bonding between carbonyl oxygen and the phenolic OH group as shown

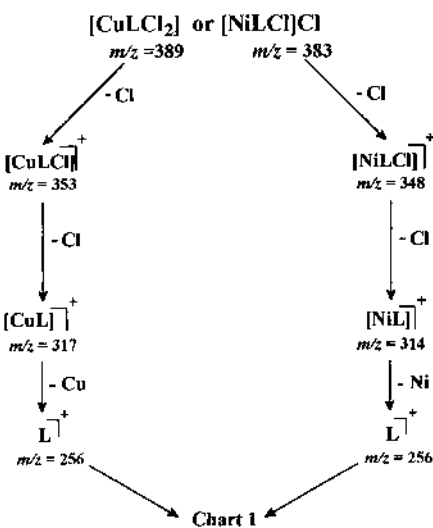
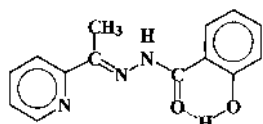


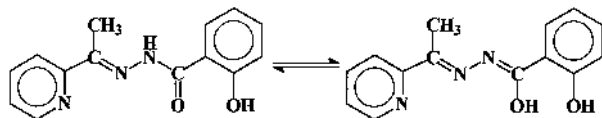
Chart 3. Proposed Fragmentation Route of  $[\text{CuLCl}_2]$  and  $[\text{NiLCl}]\text{Cl}$  Complexes

Table 2. IR Spectral Bands of APo-OHBH and Its Metal Complexes

| Compound   | $\nu(\text{OH})$ | $\nu_s(\text{NH})$ | $\nu(\text{C}=\text{O})$ | $\nu(\text{C}=\text{N})$ | $\nu(\text{C}=\text{Np})$ | $\nu(\text{C}=\text{N}^*)$ | $\nu(\text{C}-\text{O})$ | $\nu(\text{N}-\text{N})$ | $\nu(\text{M}-\text{O})$ | $\nu(\text{M}-\text{N})$ | $\nu(\text{M}-\text{Cl})$ |
|--|------------------|--------------------|--------------------------|--------------------------|---------------------------|----------------------------|--------------------------|--------------------------|--------------------------|--------------------------|---------------------------|
| L = APo-OHBH   | 3445             | 3281               | 1638                     | 1607                     | 1548                      | —                          | —                        | 985                      | —                        | —                        | —                         |
| $[\text{CoLCl}]\text{Cl}$                                    | 3450             | 3266               | 1605                     | 1600                     | 1568                      | —                          | —                        | 1015                     | 540                      | 415                      | 320                       |
| $[\text{MnLCl}]\text{Cl}$                                    | 3450             | 3262               | 1609                     | 1600                     | 1571                      | —                          | —                        | 1015                     | 544                      | 415                      | 313                       |
| $[\text{NiLCl}]\text{Cl}$                                    | 3450             | 3220               | 1622                     | 1603                     | 1574                      | —                          | —                        | 1015                     | 527                      | 420                      | 312                       |
| $[\text{CuLCl}_2]$   | 3450             | 3230               | 1625                     | 1598                     | 1560                      | —                          | —                        | 1044                     | 530                      | 438                      | 345                       |
| $[\text{HgLCl}_2]$   | 3450             | 3224               | 1655                     | 1603                     | 1563                      | —                          | —                        | 1015                     | 522                      | 430                      | 360                       |
| $[\text{Fe}(\text{L}-\text{H})\text{Cl}_2]$                  | 3450             | —                  | —                        | 1597                     | 1555                      | 1615                       | 1428                     | 1037                     | 530                      | 445                      | 355                       |
| $[\text{Ni}(\text{L}-\text{H})_2]$                           | 3447             | —                  | —                        | 1595                     | 1570                      | 1620                       | 1410                     | 1044                     | 540                      | 415                      | —                         |
| $[\text{Co}(\text{L}-\text{H})_2] \cdot 2\text{H}_2\text{O}$ | 3450             | —                  | —                        | 1595                     | 1565                      | 1620                       | 1409                     | 1045                     | 540                      | 418                      | —                         |
| $[\text{Cu}(\text{L}-\text{H})\text{OAc}]$                   | 3441             | —                  | —                        | 1600                     | 1580                      | 1630                       | 1413                     | 1040                     | 540                      | 415                      | —                         |
| $[\text{Cu}(\text{L}-\text{H})_2]$                           | 3447             | —                  | —                        | 1595                     | 1570                      | 1620                       | 1409                     | 1043                     | 540                      | 415                      | —                         |
| $[\text{Cd}(\text{L}-\text{H})_2]$                           | 3445             | —                  | —                        | 1595                     | 1570                      | 1620                       | 1410                     | 1040                     | 540                      | 435                      | —                         |

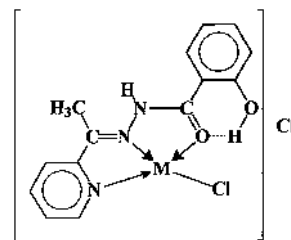


Structure I



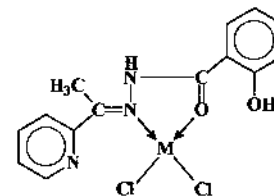
Structure II

Structure III



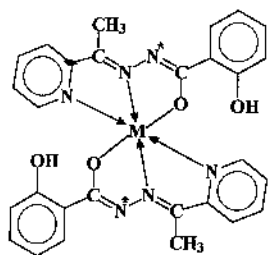
M=Mn(II), Co(II) or Ni(II)

Structure VI



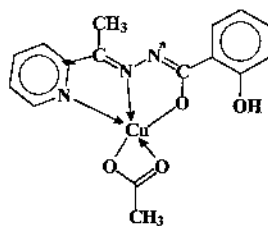
M=Cu(II) or Hg(II)

Structure VII



M=Ni(II), Co(II), Cu(II) or Cd(II)

Structure IV



Structure V

in structure I. Also, the spectrum shows a band at  $1345\text{ cm}^{-1}$  assigned to  $\delta\text{ OH}$ .<sup>20</sup> The most important assignments of the ligand and its metal complexes are recorded in Table 2.

APo-OHBH can be represented by two tautomeric forms, the keto form (structure II) and the enol form (structure III).

The IR spectrum of the APo-OHBH shows a band at  $3281\text{ cm}^{-1}$  which may be assigned to the  $\nu\text{-NH}$  of the imino group. The bands at  $1638$ ,  $1607$ ,  $1540$ ,  $1379$  and  $970\text{ cm}^{-1}$  can be, respectively, assigned to the amide (1)  $\nu(\text{C}=\text{O})$ ,  $\nu(\text{C}=\text{N})$ , amide (2)  $\delta(\text{N}-\text{H})$ , amide (3) and  $\nu\text{N}-\text{N}$  modes.<sup>21,22</sup> The bands located at  $1548$ ,  $1015$ ,  $632$  and  $410\text{ cm}^{-1}$ , may be assigned to  $\nu\text{C}=\text{C}=\text{N}_p$  of the pyridyl ring.<sup>23</sup> The ring skeletal mode, in plane ring deformation mode and out of plane ring deformation mode,<sup>24</sup> respectively, are of considerable importance in deciding whether or not the heterocyclic nitrogen is involved in the coordination with metal ion. The amide (2)  $\delta(\text{N}-\text{H})$  band shifts to lower wavenumber and its intensity is impaired partly as a result of deprotonation during complex formation.<sup>25</sup>

The azomethine band is shifted to lower frequency in all metal complexes, suggesting that this group takes part in coordination. The coordination of nitrogen to the metal atom would be expected to reduce the electron density on the azomethine link and thus cause a shift in the  $\text{C}=\text{N}$  band. The small shift to higher frequency of the band at  $985\text{ cm}^{-1}$  due to  $\nu\text{N}-\text{N}$ <sup>26</sup> can be taken as additional evidence of the participation of the azomethine group in bonding. All these changes in amide group vibrations reveal the involvement of the amide oxygen in coordination by loss of one proton. This result is confirmed by the presence of a new band at  $522-544\text{ cm}^{-1}$ , ascribed to  $\nu(\text{M}-\text{O})$ .<sup>27,28</sup>

The IR spectra of  $[\text{Cu}(\text{L}-\text{H})\text{OAc}]$ ,  $[\text{Co}(\text{L}-\text{H}_2)]\cdot 2\text{H}_2\text{O}$ ,  $[\text{Ni}(\text{L}-\text{H}_2)]$ ,  $[\text{Cu}(\text{L}-\text{H}_2)]$ ,  $[\text{Cd}(\text{L}-\text{H}_2)]$  and  $[\text{Fe}(\text{L}-\text{H})\text{Cl}_2]$  com-

plexes show that APo-OHBH behaves as mononegative tridentate ligand, coordinating through carbonyl oxygen in the enol form, azomethine nitrogen and acetyl pyridyl ring nitrogen structures IV and V. However, all the amide bands disappear from the spectra of the complexes, while new bands appear at  $1620$  and  $1412\text{ cm}^{-1}$  due to  $\nu(\text{C}=\text{N})^*$  and  $\nu(\text{C}-\text{O})$  group, respectively. This indicates transformation of the carbonyl group to the enolic form through an amide  $\rightleftharpoons$  imidol tautomerism and subsequent coordination of the imidol oxygen upon deprotonation. The band at  $1607\text{ cm}^{-1}$ , assigned to  $\nu(\text{C}=\text{N})$ , is shifted to lower frequencies in complexes which indicates the use of the azomethine group as one of the coordinating sites of the ligand. Also, the shift to higher frequency of the band at  $985\text{ cm}^{-1}$  due to  $\nu(\text{N}-\text{N})$  can be taken as additional evidence of the participation of the azomethine group in bonding. Coordination of acetylpyridyl ring nitrogen is suggested on the basis of the observed changes in the bands at  $1548$ ,  $1015$ ,  $632$  and  $410\text{ cm}^{-1}$  assigned to  $\nu\text{C}=\text{C}=\text{N}_p$  of pyridine ring, the ring skeletal mode, and in-plane ring deformation mode. These bands have been reported to be shifted to high frequencies.<sup>29</sup> The spectra of  $[\text{Cu}(\text{L}-\text{H})\text{OAc}]$  complex show two bands at  $1500$  and  $1445\text{ cm}^{-1}$  assignable to  $\nu_{\text{as}}$  and  $\nu_{\text{s}}$  of the acetate group.

The ligand functions as a neutral tridentate in manganese, cobalt and nickel chloride complexes, *via* the azomethine group, carbonyl group in the keto form and acetylpyridyl ring nitrogen as shown in structure VI.

This behaviour is supported by the following evidence: i) the negative shift of carbonyl group to lower wavenumber, ii) the shift of  $\nu(\text{C}=\text{N})$  to lower frequencies together with the shift of  $\nu(\text{N}-\text{N})$  to higher frequencies,<sup>26</sup> iii) the positive shift of the bands due to 2-acetylpyridyl ring, iv) the values of molar conductance in DMF and the number of ionizable halide ions, v) the bands at  $3445$  and  $1345\text{ cm}^{-1}$  due to  $\nu\text{OH}$  and  $\delta\text{OH}$  remain more or less unaltered, indicating that this group does not take part in coordination, and vi) the appearance of the band in the region  $312-320\text{ cm}^{-1}$  assigned to  $\nu(\text{M}-\text{Cl})$ .<sup>30</sup> On the other hand, in  $[\text{MLCl}_2]$  (where  $\text{M}=\text{Hg}(\text{II})$ )

or Cu(II) complexes, the ligand acts as a neutral bidentate through the azomethine and carbonyl groups as shown in structure VII. This mode of chelation is supported by: i) the shift of both  $\nu(\text{C}=\text{O})$  and  $\nu(\text{C}=\text{N})$  to lower wavenumbers, and ii) the  $\nu(\text{N}-\text{N})$  shifts to higher wavenumber. A band near  $300\text{ cm}^{-1}$  in the complexes is assigned to  $\nu(\text{M}-\text{Cl})$  vibration.<sup>30)</sup>

The IR spectra of all complexes exhibit several new bands in the region  $522-540$  and  $415-445\text{ cm}^{-1}$ ; these bands can be assigned to  $\nu(\text{M}-\text{O})$  and  $\nu(\text{M}-\text{N})$  vibrations, respectively.<sup>31,32)</sup>

The water of crystallisation was determined by the weight loss on heating the complex in an oven up to  $120\text{ }^\circ\text{C}$  for 2 h.

**Thermal Analysis** Thermal gravimetric analysis (TGA) and differential thermal analysis (DTA) for the complexes  $[\text{NiLCl}]\text{Cl}$  and  $[\text{CuLCl}_2]$  were studied. Both complexes display two stages of weight loss. The first decomposition process occurs at about  $397\text{ }^\circ\text{C}$  (Ni) or  $304\text{ }^\circ\text{C}$  (Cu) and is assigned to the loss of one chlorine atom for Cu-complex and two for Ni-complex. It can be seen that the complexes began to decompose exothermically at *ca.*  $421\text{ }^\circ\text{C}$  (Ni) and  $647\text{ }^\circ\text{C}$  (Cu), and the decomposition was completed at *ca.*  $515\text{ }^\circ\text{C}$  and  $675\text{ }^\circ\text{C}$  for  $[\text{NiLCl}]\text{Cl}$  and  $[\text{CuLCl}_2]$ , respectively, with the formation of metal oxides.

**Electronic Spectra and Magnetic Moments** The corrected magnetic moments at room temperature for diamagnetism are given in Table 3 with the electronic spectral data.

The electronic spectrum of  $[\text{MnLCl}]\text{Cl}$  in DMSO shows three bands at  $25445$ ,  $27855$  and  $29411\text{ cm}^{-1}$  which may assigned to  ${}^6A_1 \rightarrow {}^4E$ ,  ${}^6A_1 \rightarrow {}^4T_2$  (D) and  ${}^6A_1 \rightarrow {}^4E$  (D), respectively.<sup>33)</sup> These bands are clearly observed indicating tetrahedrally coordinated manganese.<sup>34)</sup> The  $\mu_{\text{eff}}$  value for the manganese(II) compound is expected for the high spin  $d^5$  system.

The electronic spectrum of the green  $[\text{CoLCl}]\text{Cl}$  complex in DMF exhibits one intense band at  $14793\text{ cm}^{-1}$  attributable to  ${}^4A_2(\text{F}) \rightarrow {}^4T_1(\text{P})$  transition and a shoulder at  $16474\text{ cm}^{-1}$  due to spin-coupling.<sup>35)</sup> Another weak band at  $25575\text{ cm}^{-1}$  corresponding to the transition  ${}^4A_2(\text{F}) \rightarrow {}^4T_1(\text{P})$ , indicates a tetrahedral stereochemistry for this complex. The  $\mu_{\text{eff}}$  (4.53 B.M.) is consistent with tetrahedral configuration around the Co(II) ion. The electronic spectrum of  $[\text{Co}(\text{L}-\text{H})_2] \cdot 2\text{H}_2\text{O}$  in DMSO shows two bands at  $14286$  and  $18305\text{ cm}^{-1}$  assigned to  ${}^4T_{1g}(\text{F}) \rightarrow {}^4A_{2g}(\text{F})$  ( $\nu_2$ ) and  ${}^4T_{1g}(\text{F}) \rightarrow {}^4T_{1g}(\text{P})$  ( $\nu_3$ ) transitions, respectively. There is also a shoulder at  $26178\text{ cm}^{-1}$  being attributed to spin-orbital coupling effects or to transition to the doublet state.<sup>31)</sup> The molecular extinction coefficient ( $\epsilon$ ) for  $\nu_2$  ( $161\text{ mol}^{-1}\text{ cm}^{-1}$ ) is consistent with octahedral geometry, as are the calculated values of  $D_q$ ,  $B$  and  $\beta$  using the Tanabe-Sugano diagram.<sup>36)</sup>

The electronic spectrum of  $[\text{Ni}(\text{L}-\text{H})_2]$  in DMSO is con-

sistent with octahedral geometry showing three  $d-d$  transitions bands at  $11792$ ,  $16792$  and  $21276\text{ cm}^{-1}$  assignable to  ${}^3A_{2g} \rightarrow {}^3T_{2g}$  ( $\nu_1$ ),  ${}^3A_{2g} \rightarrow {}^3T_{1g}(\text{F})$  ( $\nu_2$ ) and  ${}^3A_{2g} \rightarrow {}^3T_{1g}(\text{P})$  ( $\nu_3$ ) transitions, respectively. The value of the molecular extinction coefficient ( $\epsilon$ ) for  $\nu_2$  ( $391\text{ mol}^{-1}\text{ cm}^{-1}$ ), the value of magnetic moment (3.21 B.M.) and the calculated values of  $D_q$ ,  $B$  and  $\beta$  are also consistent with the octahedral geometry.<sup>33)</sup> The electronic spectrum of  $[\text{NiLCl}]\text{Cl}$  is consistent with tetrahedral geometry showing one band at  $14286\text{ cm}^{-1}$  assignable to  ${}^3T_1(\text{F}) \rightarrow {}^3T_1(\text{P})$  ( $\nu_3$ ) transition and a band at  $22222\text{ cm}^{-1}$  assignable to charge-transfer.<sup>37)</sup> The value of the molecular extinction coefficient ( $\epsilon$ ) for  $\nu_3$  ( $2101\text{ mol}^{-1}\text{ cm}^{-1}$ ), the value of magnetic moment (3.5 B.M.,  $\lambda = -151\text{ cm}^{-1}$ ) and the calculated ligand field parameters  $D_q$ ,  $B$  and  $\beta$  are also consistent with tetrahedral geometry.<sup>36)</sup>

The magnetic moments of  $[\text{Cu}(\text{L}-\text{H})\text{OAc}]$  and  $[\text{CuLCl}_2]$  are in the range expected for copper(II) complexes having monomeric structures.<sup>38)</sup> The electronic spectra of the copper(II) complexes show a broad band centered at  $14492$  and  $13736\text{ cm}^{-1}$ , respectively, which may be due to a combination of the  ${}^2B_{1g} \rightarrow {}^2A_{1g}$  and  ${}^2B_{1g} \rightarrow {}^2E_g$  transitions in a square-planar configuration.<sup>36)</sup> However, the bands observed at  $25380$  and  $24752\text{ cm}^{-1}$ , respectively, may be due to charge-transfer.<sup>39)</sup> The magnetic moment values (Table 3) corresponding to the spin-only value for one unpaired electron fall in the range normally observed for Cu(II) complexes having an orbitally non-degenerate  $B_{1g}$  ground state, thereby indicating no metal-metal interaction.<sup>39)</sup>

**Antimicrobial Activity** From the data of Table 4, the order of antibacterial activity of the previously reported<sup>12,13)</sup> ligands and (APo-OHBH) ligand under investigation vary greatly with the type of organic ligand and/or of metal cations. The order of the activity of the organic ligands against gram-negative bacteria (*E. coli*) may be represented by the following sequence: AABH > HPo-OHBH > AAOHBH while the sequence: AAOHBH > HPo-OHBH > AABH represents the activity of the organic ligands against gram-positive (*B. subtilis*) bacteria. It is clear that the OH phenolic and pyridyl ring play an important role in the antibacterial activity, and the activity of the ligands against *B. subtilis* seems dependent on the presence of a substituent on the phenyl ring, while the activity of the ligand against *E. coli* seems independent of the presence of a phenyl ring substituent. It is known that the ligands which include oxygen, nitrogen or sulfur as the binding atoms are those typically found in molecules of biological interest.<sup>40)</sup> The antimicrobial activity of the APo-OHBH ligand and its metal complexes show antibacterial activity against both *E. coli* and *B. subtilis*. It seems that copper(II) and mercury(II) complexes

Table 3. Electronic Spectral and Magnetic Data of APo-OHBH Complexes

| Compound   | Band position<br>( $\text{cm}^{-1}$ ) | $\epsilon$<br>$1\text{ cm}^{-1}\text{ mol}^{-1}$ | $D_q$  | $B$   | $\beta$ | $\mu_{\text{eff}}$ (B.M.) |
|--|---------------------------------------|--|--------|-------|---------|---------------------------|
| $[\text{MnLCl}]\text{Cl}$                                    | 25445, 27855, 29411                   | —  | —      | —     | —       | 5.78                      |
| $[\text{CoLCl}]\text{Cl}$                                    | 14793, 16474, 25575                   | $2.9 \times 10^2$                                | 827.7  | 429.2 | 0.44    | 4.53                      |
| $[\text{Ni}(\text{L}-\text{H})_2]$                           | 11792, 16792, 21276                   | 39   | 1007.6 | 522.5 | 0.50    | 3.21                      |
| $[\text{CuLCl}_2]$   | 13736, 24752                          | 131  | —      | —     | —       | 1.74                      |
| $[\text{Cu}(\text{L}-\text{H})\text{OAc}]$                   | 14492, 25380                          | 152  | —      | —     | —       | 1.83                      |
| $[\text{Co}(\text{L}-\text{H})_2] \cdot 2\text{H}_2\text{O}$ | 14286, 18305, 26178                   | 16   | 764.5  | 844.4 | 0.87    | 3.42                      |
| $[\text{NiLCl}]\text{Cl}$                                    | 14286, 22222                          | 210  | —      | —     | —       | 3.5                       |

Table 4. Antimicrobial Activity of APo-OHBH Ligand and Its Metal Complexes

| Compound                                  | Actual inhibition zone diameter (mm) | Actual inhibition zone diameter (mm) | References |
|---|--------------------------------------|--------------------------------------|------------|
|   | <i>Escherichia Coli</i>              | <i>Bacillus Subtilis</i>             |            |
| APo-OHBH5L                                | 22                                   | 6                                    | This work  |
| [Cu(L-H)OAc]                              | 17                                   | 22                                   | This work  |
| [Co(L-H) <sub>2</sub> ]·2H <sub>2</sub> O | 7                                    | 18                                   | This work  |
| [Ni(L-H) <sub>2</sub> ]                   | 0                                    | 4                                    | This work  |
| [MnLCl]Cl                                 | 2                                    | 22                                   | This work  |
| [HgLCl <sub>2</sub> ]                     | 17                                   | 21                                   | This work  |
| AAOHBH                                    | 2                                    | 16                                   | 13         |
| Cu(L-H)OAc]·H <sub>2</sub> O              | 16                                   | 1                                    | 13         |
| [Co(L-H)OAc]·H <sub>2</sub> O             | 2                                    | 4                                    | 13         |
| [Ni(L-H)OAc]·2H <sub>2</sub> O            | 0                                    | 0                                    | 13         |
| AABH                                      | 7                                    | 2                                    | 12         |
| [Cu(L-H)OAc]                              | 0                                    | 4                                    | 12         |
| [Co(L-H)OAc]·H <sub>2</sub> O             | 0                                    | 4                                    | 12         |
| [Ni(L-H)OAc]                              | 4                                    | 3                                    | 12         |
| Erythromycin                              | 0                                    | 19                                   | 41         |
| Ampicillin                                | 0                                    | 16                                   | 41         |

show higher activity against both bacteria, comparable to that of the antibacterial drugs on the market,<sup>41)</sup> AABH, AAOHBH ligands and its metal complexes.<sup>12,13)</sup> The antibacterial results of *cis*-configured chloro complexes [CuLCl<sub>2</sub>] and [HgLCl<sub>2</sub>] on the growth of *E. coli* and *B. subtilis* bacteria may be caused by the inhibition of cell reproduction without simultaneous inhibition of bacterial growth which eventually leads to the formation of long, filamentous cells. It has been observed that trace amounts of *cis*-configured chloroplatinum(II) was responsible for this biological effect<sup>42)</sup> comparable to that serendipitously discovered by B. Rosenberg *et al.* in the 1960s.<sup>43)</sup> The observed filamentous growth of bacteria indicates the potential antibacterial activity of the corresponding substances *via* an inhibition of cell division (cytostatic effect). The square-planer of *cis*-configured complexes [CuLCl<sub>2</sub>] and [HgLCl<sub>2</sub>] show higher activity due to the presence of labile *cis*-chlorine. This liability is essential to exhibit an intermediate bond stability with metal and thus is exchangeable on a physiological time-scale. Complexes with very labile ligand X (X is halides, aqua, hydroxo, *etc.*) are toxic while very inert M-X bonds render the corresponding substances inactive.<sup>44)</sup> As a rule, active complexes are neutral and may initially penetrate cell membranes more easily than charged compounds.<sup>44)</sup> From the data, there is a great difference observed between [Co(L-H)<sub>2</sub>] and [Ni(L-H)<sub>2</sub>] although both complexes possess similar structures. The octahedral complex of [Ni(L-H)<sub>2</sub>] seems without activity against both *E. coli* and *B. subtilis* comparable to the octahedral structure of [Co(L-H)<sub>2</sub>]. This behaviour was confirmed long ago, nickel has been the only element of the 'late' 3d transition metals for which a biological role has not been definitely established. The reasons for this are manifold: nickel ions do not exhibit a very characteristic light absorption in the presence of physiologically relevant ligands.<sup>44)</sup> Moreover, the same behaviour was confirmed by our previous results.<sup>12,13,45)</sup>

**Dedication** To the memory of the late Prof. M. A. Khat-tab.

#### References

1) Hoi N. P., *J. Chem. Soc.*, **1953**, 1358.

- 2) Craig J. C., Edger J., *Nature* (London), **34**, 176 (1955).
- 3) Mohan M., Kumar A., Kumar M., *Inorg. Chim. Acta*, **136**, 65 (1987) and refs. therein.
- 4) Sastry P. S. S. J., Rao T. R., *Proc. Indian Acad. Sci. (Chem. Sci.)*, **107**, 25 (1995).
- 5) Tsukamoto Y., Sato K., Tanaka K., Yanai T., *Bioscience Biotech. Biochem.*, **61**, 304 (1997).
- 6) Keefe G. P., *Can. Vet. J.*, **38**, 429 (1997).
- 7) Constable E. C., Khan F. K., Lewis J., Liptrot M. C., Raith P. R., *J. Chem. Soc., Dalton Trans.*, **1985**, 333.
- 8) Wu J. G., Deng R. W., Chen Z. N., *Transition Met. Chem.*, **18**, 23 (1993).
- 9) Takahama U., *Physiologia Plantarum*, **98**, 731 (1996).
- 10) Nawar N., Khattab M. A., Bekheit M. M., El-Kaddah A. H., *Synth. React. Inorg. Met.-Org. Chem.*, **24**, 1281 (1994).
- 11) Nawar N., Khattab M. A., Bekheit M. M., El-Kaddah A. H., *Indian J. Chem.*, **35A**, 308 (1996).
- 12) Nawar N., Khattab M. A., Hosny N. M., *Synth. React. Inorg. Met.-Org. Chem.*, **8**, (1999) accepted.
- 13) Nawar N., Hosny N. M., *Transition Met. Chem.*, (1999) accepted.
- 14) Vogel A. I., "A text book of Quantitative Inorganic Analysis," Longmans, London, 2nd ed., 1961.
- 15) Gerhardt P., "Manual of Methods for General Bacteriology," Castello, American Society for Microbiology, 1981.
- 16) Geary W. J., *Coord. Chem. Rev.*, **7**, 81 (1971).
- 17) La Planche L. A., Rogers M. T., *J. Am. Chem. Soc.*, **86**, 337 (1964).
- 18) Patel S. A., Kulkarni V. H., *Inorg. Chim. Acta*, **95**, 195 (1984).
- 19) Rao T. R., Srivastava M. R., *Bull. Chem. Soc. Jpn.*, **65**, 2766 (1992).
- 20) Looker J. H., Hanneman W. W., *J. Org. Chem.*, **27**, 381 (1962).
- 21) Figgins P. E., Busch D. H., *J. Phys. Chem.*, **65**, 2236 (1961).
- 22) Rana V. B., Sahni S. K., Gupta S. P., Songal S. K., *J. Inorg. Nucl. Chem.*, **69**, 1098 (1977).
- 23) Alpert N. L., Keiser W. E., Szymanski H. A., "Theory and Practical of Infrared Spectroscopy," Plenum, New York, 1970.
- 24) Sakamoto M., *Inorg. Chim. Acta*, **131**, 139 (1987).
- 25) Bellamy L. J., "Advance in Infrared Group Frequencies," Methuen, 1969, p. 2.
- 26) Sathyanarayana D. N., Nicholls D., *Spectrochim. Acta*, **34A**, 263 (1978).
- 27) Nakamoto K., "Infrared and Raman Spectra of Inorganic and Coordination Compounds," 4th ed., Wiley, New York, 1986, p. 232.
- 28) Teotia M. P., Singh I., Singh P., Rana V. B., *Synth. React. Inorg. Met.-Org. Chem.*, **14**, 603 (1984).
- 29) Banner J. D., Singh I. P., *Indian J. Chem.*, **6**, 34 (1968).
- 30) Nakamoto K., "Infrared and Raman Spectra of Inorganic and Coordination Compounds," 2nd ed., Wiley, New York, 1971, p. 167.
- 31) Speca A. N., Karayani N. M., Pytlewski L. L., *Inorg. Chim. Acta*, **9**, 87 (1974).
- 32) Beecroft B., Compbell M. J. M., Grzeskowiak R., *J. Inorg. Nucl. Chem.*, **36**, 55 (1974).
- 33) Nickolls D., "Complexes and First-Row Transition Elements," Macmillan, Great Britain, 1974, p. 97.
- 34) Vdovenko V. M., Skoblo A. T., Serglobov, *Radio Khimiya*, **8**, 651 (1966).
- 35) Panda A. K., Mishra S. B., Mohapatra B. K., *J. Inorg. Nucl. Chem.*, **42**, 497 (1980).
- 36) Lever A. B. P., "Inorganic Electronic Spectroscopy," Elsevier, Amsterdam, 1968, p. 318.
- 37) West D. X., El-Sawaf A. K., Bain G. A., *Transition Met. Chem.*, **23**, 1 (1998).
- 38) Palla G., Pelizzi C., Predieri G., Vignali C., *Gazz. Chim. Italiana*, **112**, 339 (1982).
- 39) El-Asmy A. A., Shaibi Y. M., Shedaiwa I. M., Khattab M. A., *Synth. React. Inorg. Met.-Org. Chem.*, **20**, 461 (1990).
- 40) Mahler H. R., Cordes E. H., "Biological Chemistry," Harper & Row, New York, 1971, p. 17.
- 41) Hammond S. M., Lambert P. A., "Antibiotics and Antimicrobial Action," Arnold, Great Britain, 1981.
- 42) Umopathy P., *Coord. Chem. Rev.*, **95**, 129 (1989).
- 43) Rosenberg B., Comp L. Van, Krigas T., *Nature* (London), **205**, 698 (1965).
- 44) Kaim W., Schwederski B., "Bioinorganic Chemistry: Inorganic Elements in the Chemistry of Life," Wiley, New York, 1996, p. 362, 366, 372, 172.
- 45) Nawar N., Hosny N. M., in preparation.